Section A. Film dewetting at temperatures above the T_g of PS

Figure S1. A plot of the intensity of the Si^+ ion ($I(Si^+)$) normalized with respect to the total ion intensity (I_T) of 120-nm polymer films of different molecular weights as a function of the annealing temperature. T_D denotes the dewetting temperature (which is defined by the dotted line as shown in the figure, where an abrupt change of the $I(Si^+)/I_T$ occurs) and Tg is the bulk glass transition temperature.

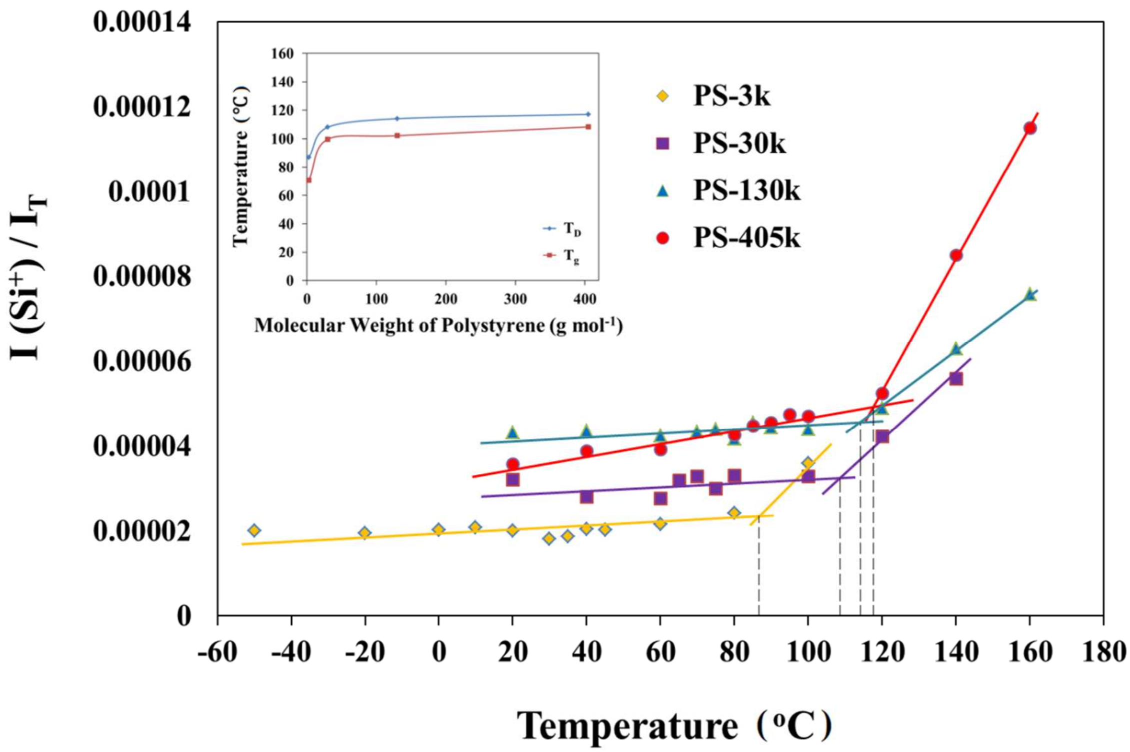

The Si^+ ion is related to the silicon wafer substrate and the presence of the Si^+ ion indicates the exposure of the substrate of the PS thin film. The Si^+ ion intensity is negligible at temperatures below the T_g, implying that the thin films were homogenous and free of crack. However, an abrupt increase of the Si^+ ion intensity occurred at high temperatures, indicating occurrence of film dewetting. The dewetting temperature was about 10 to 20 ^oC higher than the bulk T_g. In the PCA calculation, all ToF-SIMS data obtained at temperatures below T_D were chosen to exclude spectra of dewetted films.

Section B. A positive ion spectrum of the 120-nm thick PS-405k film

Figure S2. A positive ion spectrum of the 120-nm thick PS-405k film obtained at room temperature. C_n denotes the cluster of hydrocarbon with n carbons.

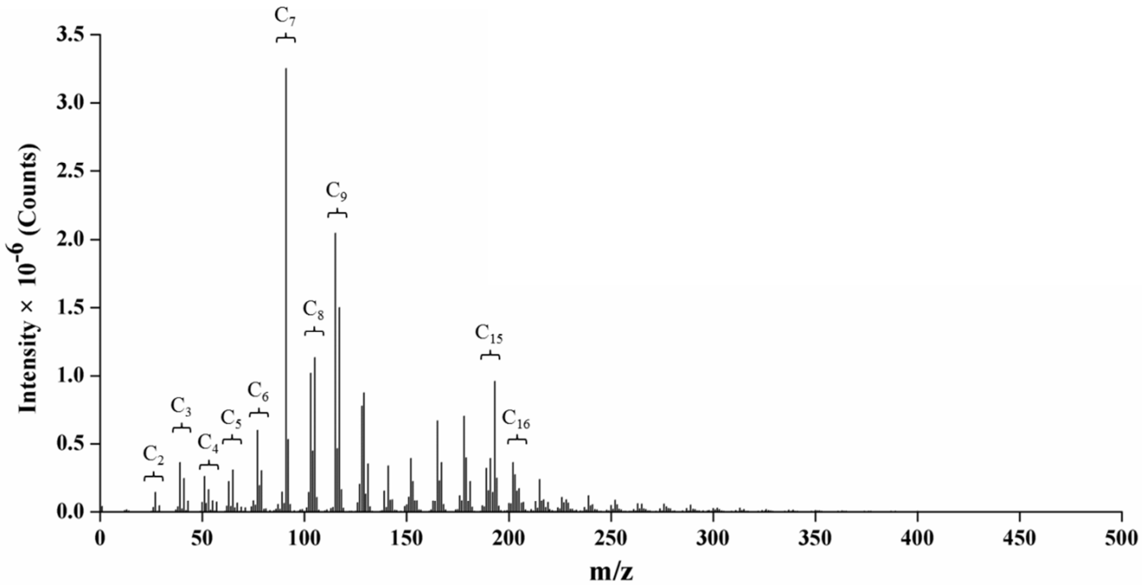

The positive ion spectrum of PS obtained at room temperature bears a close resemblance to those shown in the literature. Particularly, the observed fragment ions consist of both low-mass aliphatic hydrocarbon ions, such as $C_2H_3^+$, $C_3H_3^+$, $C_4H_3^+$, $C_4H_9^+$, and $C_5H_5^+$, and high-mass aromatic hydrocarbon ions, such as $C_7H_7^+$, $C_8H_7^+$, $C_9H_7^+$, $C_{15}H_{13}^+$, and $C_{16}H_{13}^+$.

Section C. PCA results of spectra of PS-405k with and without the high-intensity ion peaks such as $C_7H_7^+$, $C_9H_7^+$ and $C_9H_9^+$

Figure S3: PCA of the ToF-SIMS spectra of PS-405k thin films (120-nm thick) at temperatures ranging from room temperature to 100 ^oC: (a) A PCA scores plot of a total of 16 positive ion mass spectra acquired at 8 different temperatures (after deletion of $C_7H_7^+$, $C_9H_7^+$, and $C_9H_9^+$); (b) the corresponding loadings plot of the positive ions; (c) A PCA scores plot of original data without any deletion; (b) the corresponding loadings plot of the positive ions. Inclusion of these high-intensity ion peaks was shown not to affect the outcomes of the scores plot but allowed the identification of the low-intensity characteristic ion peaks.

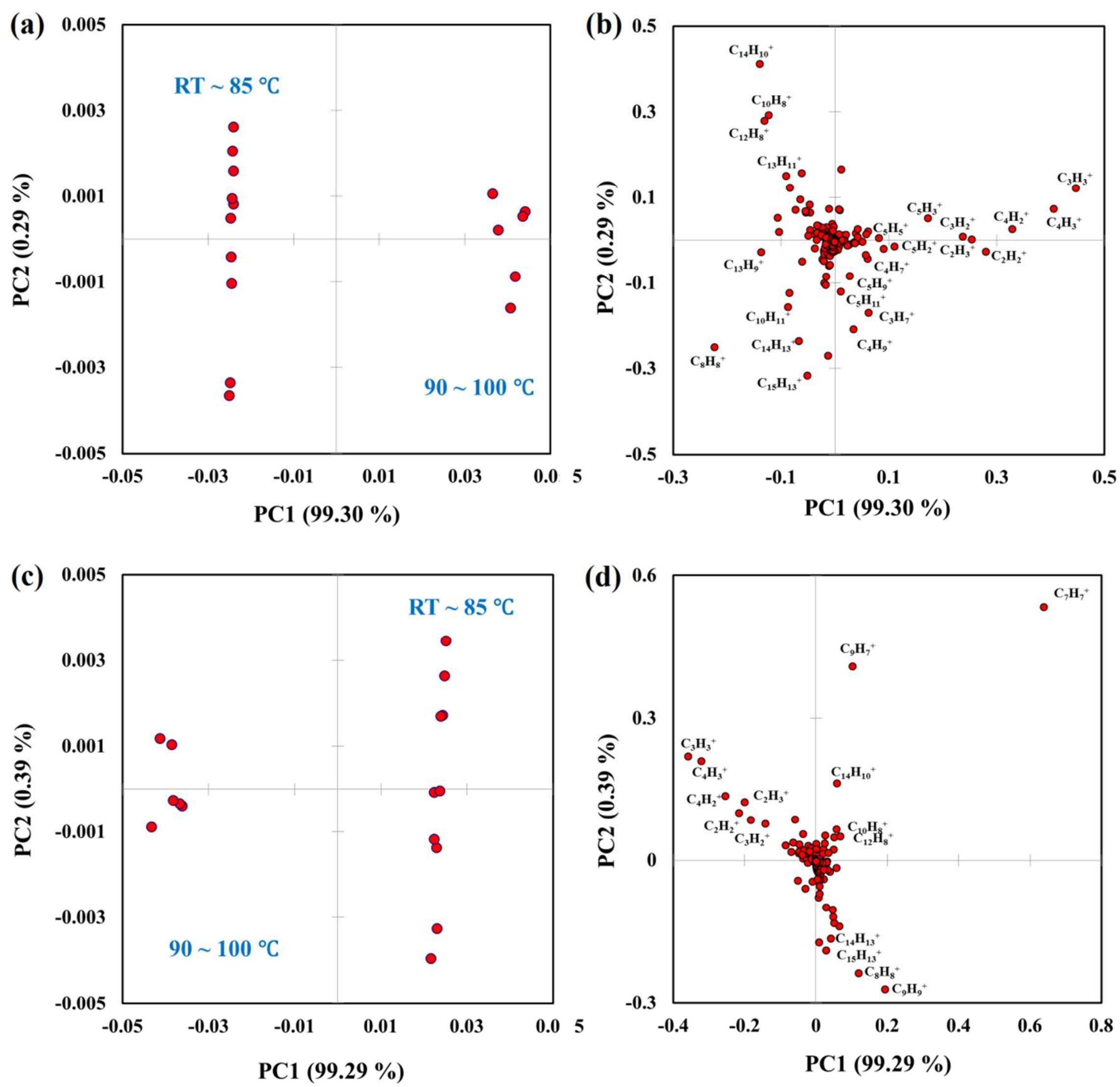

Section D.

Figure S4: A PCA scores plot of positive ion mass spectra acquired from the surface of PS thin films (120-nm thick) with four different molecular weights at various temperatures. The data points associated with the sample of each molecular weight are of different temperatures in spite of the fact that they are presented by the same color. A PCA of ToF-SIM spectra of PSs with different molecular weights shows that the effects of molecular weight are much more significant than those of temperature.

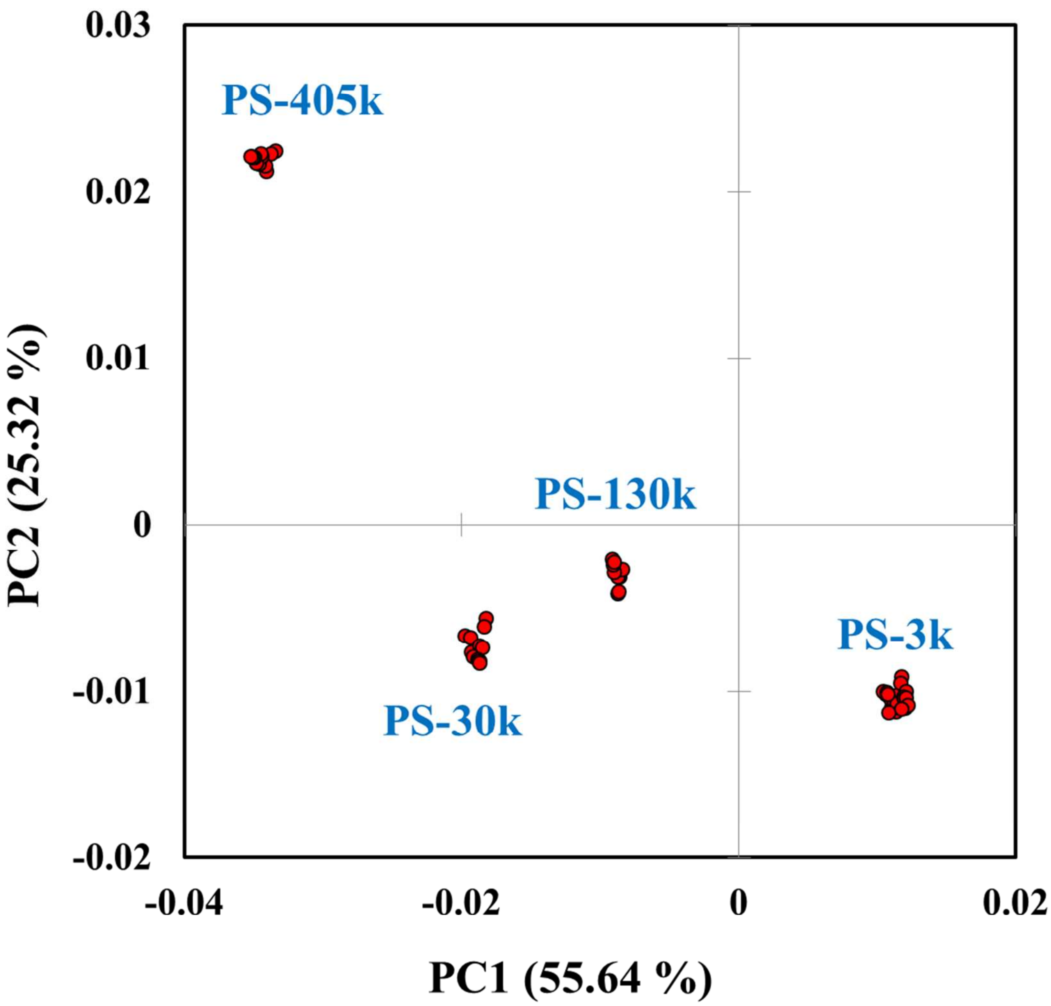

Section E. PCA results of positive ion spectra of the 120-nm thick PS-30k and PS-130k thin films

Figure S5. Results acquired from the surfaces of the PS-30k thin films (120-nm thick) at temperatures ranging from room temperature to 100 ^{o}C: (a) A PCA scores plot of a total of 16 positive ion mass spectra acquired at eight different temperatures (after normalization and mean-centering); and (b) the corresponding loadings plot of the positive ions.

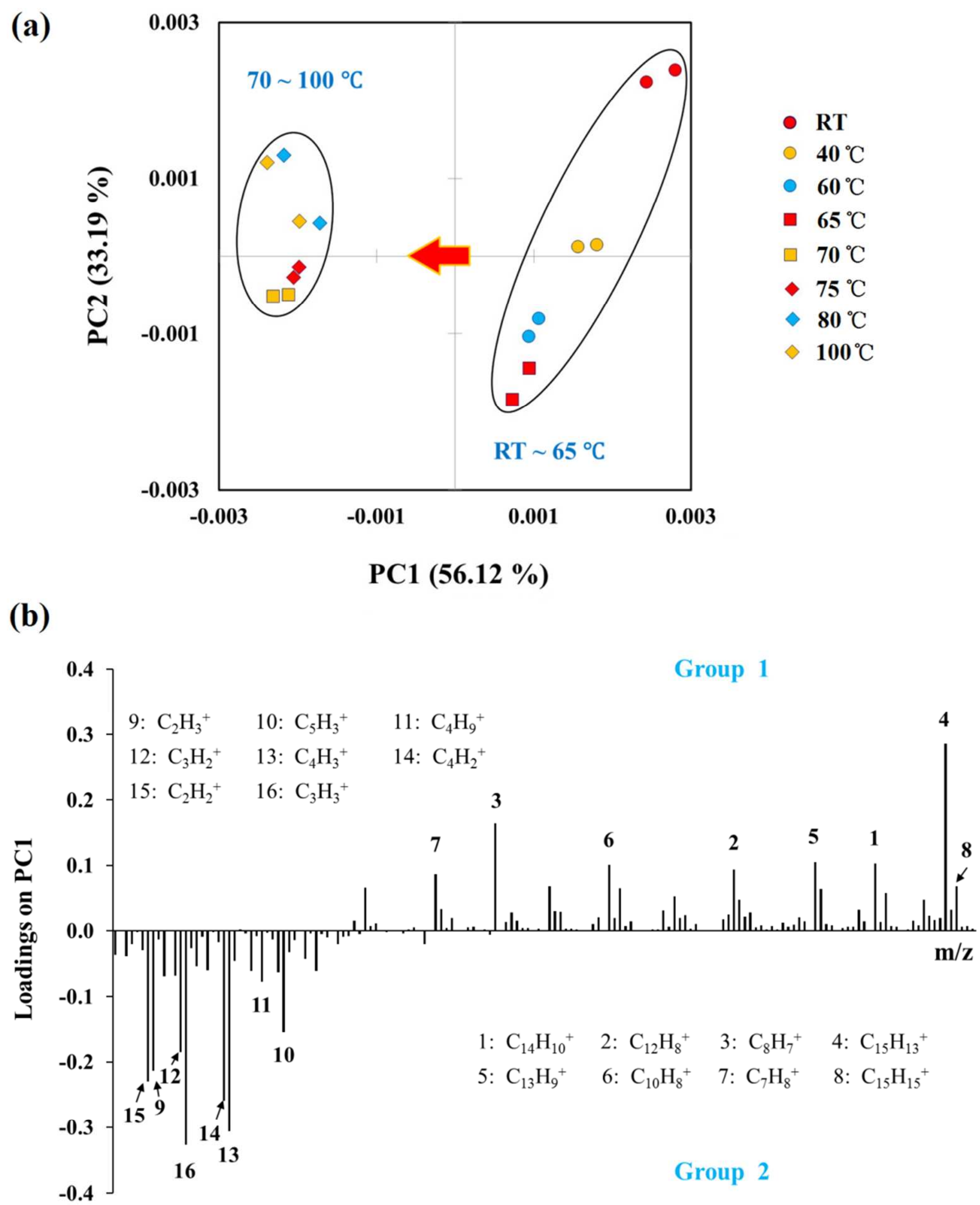

Figure S6. Results acquired from the surfaces of the PS-130k films (120-nm thick) at temperatures ranging from room temperature to 100 ^{o}C: (a) A PCA scores plot of a total of 18 positive ion mass spectra acquired at 9 different temperatures (after normalization and mean-centering); and (b) the corresponding loadings plot of the positive ions.

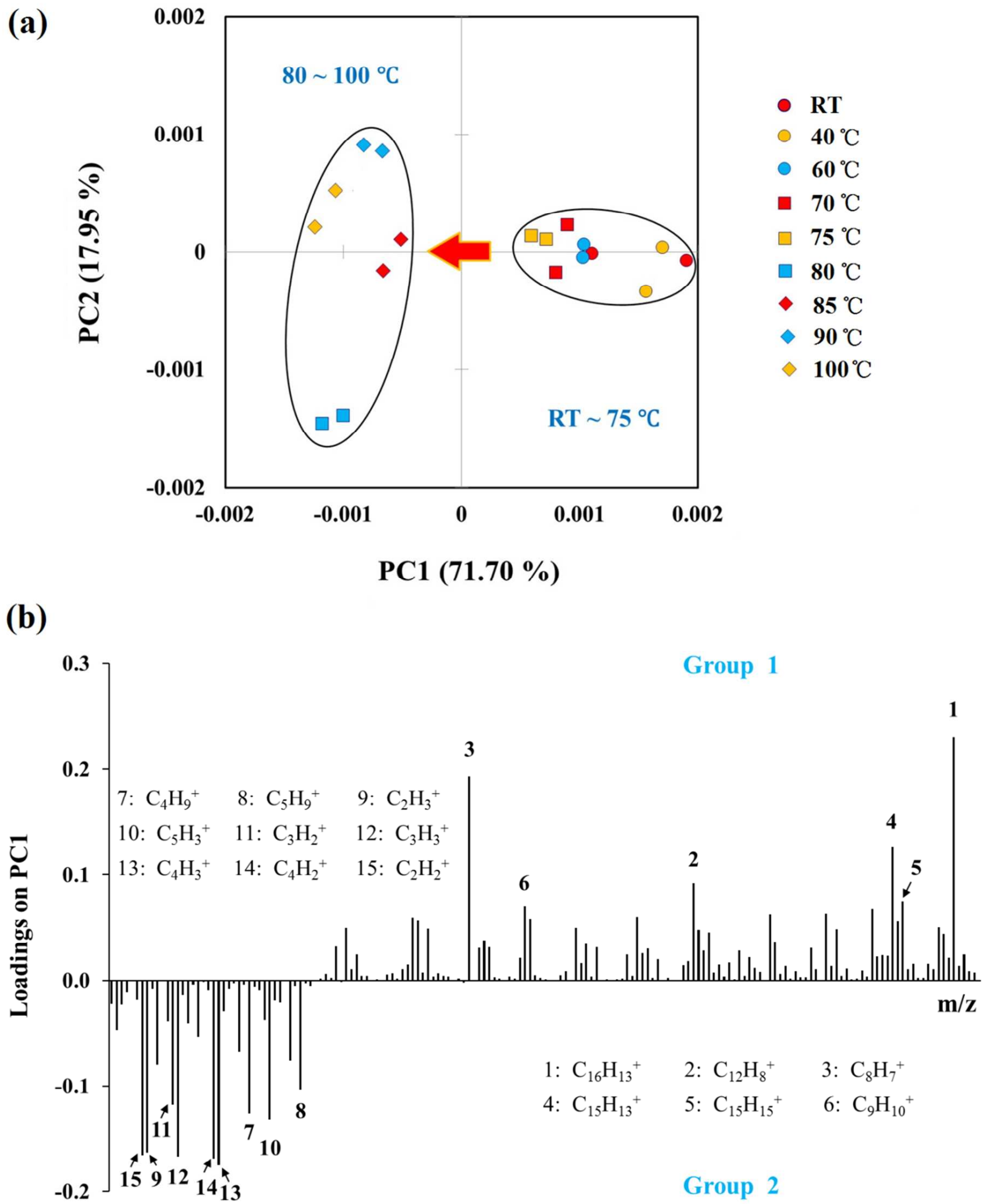

Figures S5 and S6 show PCA scores plots of the positive spectra of the PS-30k and PS-130k films at different temperatures. The data points were divided into two different groups according to their PC1 values: group 1 consists of the spectra obtained at temperatures below T_T and group 2 consists of the spectra obtained at temperatures above T_T. The results show that the fragment ions of $C_8H_8^+$, $C_{10}H_8^+$, $C_{12}H_8^+$, and $C_{14}H_{10}^+$, which are typical high-mass aromatic hydrocarbon ions, are distinctively associated with group 1; while group 2 largely contains typical low-mass aliphatic hydrocarbon ions such as $C_2H_2^+$, $C_3H_3^+$, $C_4H_9^+$ and $C_5H_7^+$.

Section F. Identities of representative fragment ions

Table S1. Chemical structures of characteristic fragment ions of PS thin films obtained from the PCA of ToF-SIMS spectra. Group 1 consists of spectra obtained at temperatures below T_T and group 2 consists of spectra obtained at temperatures above T_T.

(a) Temperature Group 1

$C_8H_8^+$ (104)	$C_9H_{10}^+$ (118)	$C_{10}H_7^+$ (127)	$C_{10}H_8^+$ (128)	$C_{11}H_7^+$ (139)
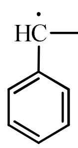	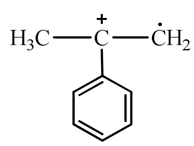	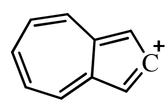	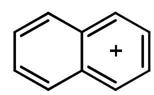	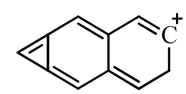
$C_{11}H_9^+$ (141)	$C_{12}H_8^+$ (152)	$C_{13}H_9^+$ (165)	$C_{14}H_{10}^+$ (178)	$C_{15}H_{13}^+$ (193)
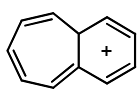	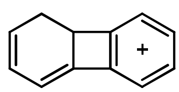	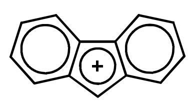	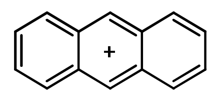	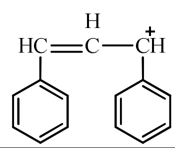

(b) Temperature Group 2

$C_2H_2^+$ (26)	$C_2H_3^+$ (27)	$C_2H_5^+$ (29)	$C_3H_2^+$ (38)	$C_3H_3^+$ (39)
$H\dot{C}{=}CH^+$	$H_2C{=}CH^+$	$H_3C{-}CH_2^+$	$H\dot{C}{=}C{=}CH^+$	$H_2C{=}C{=}CH^+$
$C_3H_5^+$ (41)	$C_3H_7^+$ (43)	$C_4H_2^+$ (50)	$C_4H_3^+$ (51)	$C_4H_5^+$ (53)
$H_2C{=}C^+{-}CH_3$	$H_2C{=}C^+{-}CH_3$	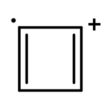	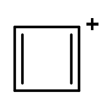	$HC{\equiv}C{-}\overset{H^+}{C}{-}CH_3$
$C_4H_7^+$ (55)	$C_4H_9^+$ (57)	$C_5H_3^+$ (63)	$C_5H_5^+$ (65)	
$H_2C{=}\underset{H}{C}{-}\overset{H^+}{C}{-}CH_3$	$H_3C{-}\overset{H_2}{C}{-}\overset{H^+}{C}{-}CH_3$	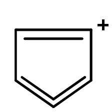	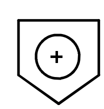	
$C_5H_7^+$ (67)	$C_5H_9^+$ (69)	$C_5H_{11}^+$ (71)		
$(H_3C)_2C^+{-}C{\equiv}CH$	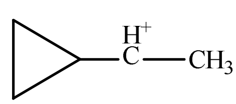	$H_3C{-}\overset{H_2}{C}{-}\overset{H^+}{C}{-}\overset{H_2}{C}{-}CH_3$		

The results show that the fragment ions are typical high-mass aromatic hydrocarbon ions, such as $C_8H_8^+$, $C_{10}H_8^+$, $C_{12}H_8^+$, and $C_{14}H_{10}^+$, which are distinctively associated with group 1. While group 2 largely contains typical low-mass aliphatic hydrocarbon ions, such as $C_2H_2^+$, $C_3H_3^+$, $C_4H_9^+$ and $C_5H_7^+$.